Evaluation of Interphase Drag Models for the Determination of Gas Hold-Up of an Air-Water System in a Spouted Bed using CFD

Jaime. A. Riera Ortiz [1], Susana Zeppieri [2,4], Luis Rojas-Solorzano[3] Sylvana Derjani-Bayeh [1].

[1]TADiP Group, Department of Thermodynamics and Transport Phenomena, [2]Transport Phenomena Group, Department of Thermodynamics and Transport Phenomena, [3]Department of Energy Conversion and Transport, Simón Bolívar University, AP89000, Caracas 1081, Venezuela.

[4] Corresponding author. E-mail:zeppieri@usb.ve; Tel.: +58-212-9063758; Fax: +58-212-9063743.

Abstract: The hydrodynamics of a dispersed air-water system within a spouted column with a concentric draft tube and a conical base is simulated using CFD based on a two–fluid Euler–Euler (E-E) modeling framework and k-ε two-equation turbulence closures. The interaction between the dispersed gas phase and the continuous liquid phase is characterized by bubble–liquid interphase forces (drag, turbulent dispersion and lift forces). The Ishii-Zuber drag model [1] and Grace adjusted drag model [2], the latter represented by: $C_D^{Grace,dense} = \upsilon_g^p C_D^{Grace}$, are compared for their capability to match experimental gas hold- up. Numerical results of Reynolds-averaged

Navier-Stokes equations with k-ε two-equation turbulence closures models when compared with Pironti experimental data [3] indicated that both drag models, predicted the air hold-up within experimental error. Furthermore, Ishii-Zuber liquid-gas drag model consistently provided better agreement of experimental results; it correctly determines the hold-up within 0.14%. Numerical agreement with adjusted Grace liquid-gas drag model, is exponent dependent $(4 \le p \le -0.5)$, turning down that the best computed hold-up is within 0.44%. for $p = 0.5$.

Keywords: CFD, Interfacial drag models, Holdup, Spouted bed column, k-ε.

1. Introduction

In a variety of chemical, biochemical, pharmaceutical and petrochemical processes, bubble columns are the reactors of choice. The bubble driven gas-liquid flow is the basis of fluid movement, providing the necessary turbulence to reach the high mixing and high interfacial area between the phases thus, improving heat and mass transfer in multiphase flow without moving parts, and having the extra benefit of low operating costs. Knowledge of the prevalent hydrodynamics behavior at each flow regimes (i.e., bubbling, slugging, etc.) is needed to better understand the effect on the mass, heat and momentum transfer between the phases, the operating and design variables that are necessary to develop scale-up strategies [4].

The two phase bubbly reactor generally is well represented with the two-fluid Euler-Euler (E-E) modeling framework. The two-fluid Euler-Euler (E-E) has shown to be numerically efficient, particularly in domains with high concentration of the dispersed phase. The momentum and

continuity of each phase with its characteristic flow properties are based on the solution of the ensemble-averaged Navier-Stokes and continuity equations. The most implemented closure model for turbulence is the k–ε because it is computationally and numerically efficient, with enough accuracy [5,6]. Riera et al. [7] applied both the k–ε and k–ω turbulence closure models in the simulation of 3D air-water system of a spouted column with a concentric draft tube and a conical base. They found no significant differences in determining air hold-up when using both closures. Regarding the geometry (cylindrical or rectangular), and dimensions, results [5,8] indicated that the 3D simulation provides a better insight of the physics of the two-phase bubble column, since 1D and 2D simulations lack of accuracy when describing this type of flow.

The ability to predict the interfacial forces between phases is very significant in analyzing a dispersed two phase system under steady or transient conditions. Inter-phase forces should be specified to close the momentum conservation equation. The prediction of the interfacial forces between the dispersed gas phase and the continuous liquid phase is dependent on semi-empirical correlations for interphase forces (e.g. drag, lift and added mass forces, i.e., virtual mass and close-to-wall lift and lubrication forces) and turbulence in the hydrodynamic column. The liquid drag force represents the primary driving force in the movement of dispersed bubbles, drops and particles using two-phase flow model. Therefore, the correct modeling of interphase forces and turbulence is fundamental to correctly describe the observed physical phenomena of the bubble column [9].

This work presents a computational fluid dynamics (CFD) simulation of the hydrodynamics of

an air-water system in a spouted column with a concentric draft tube with a conical base, in a 3D cylindrical geometry. (CFD) is a powerful tool to analyze the flow pattern in bubble columns. The two-fluid Euler–Euler modeling framework with k-ε two-equation turbulence closures is assumed to simulate the dispersed gas–liquid flows within the reactor.. The interaction between the dispersed gas phase and the continuous liquid phase is characterized by bubble–liquid interphase forces (drag force, turbulent dispersion force and lift forces). The Ishii-Zuber drag model [1] and Grace adjusted Drag model [2], $C_D^{Grace,dense} = \upsilon_g^p C_D^{Gracee}$ are compared for their capability to determine experimental gas hold-up. Numerical results of Reynolds-averaged Navier-Stokes (RANS) equations using the k-ε two-equation turbulence closure models are compared with Pironti hold-up experimental data [3].

2. Theory

2.1 Two-Fluid Euler-Euler (E-E) Model

The mathematical description of dispersed bubbly flows of air-water system is based on the two-fluid Euler-Euler approach. The two-phase flow model first assumes that the dispersed gas phase and the continuous liquid phase can be described as continua, which mean that the bubble is treated as a continuous medium with properties analogous to those of a fluid. The two-fluid modeling framework, also assumes interpenetrating fluids, meaning that the volume fraction of each fluid in space and time add up to one. The phases are separated by an interface, and the interface is treated as a surface. At the interface, jump conditions for the conservation of mass and momentum need to be formulated [1].

The two-phase flow model applied to bubble flow, also assumes isothermal conditions; no mass transfer between the two phases; the gas density ρ_g vary with pressure according to ideal gas law, $\rho_g = \frac{P}{RTo}$, liquid density ρ_l is constant. Negligible Bubble coalescence and re-dispersion, these imply that: each class of bubbles and groups of bubble of constant mass conserve their mass as long as they are in the two-phase flow produced [10].

Then the two flow Eulerian modeling framework leads to ensemble averaged mass and momentum transport equations for all phases, so for the two-phase flow under investigation a set of two continuity and two Navier-Stokes equations. The time-averaged continuity without mass transfer and momentum transfer equations for phase q, [6] can be written as:

$$\frac{\partial}{\partial t}(\upsilon_q \rho_q) + \nabla \cdot \left(\upsilon_q \rho_q \vec{u}_q\right) = 0 \tag{1}$$

$$\frac{\partial}{\partial t}(\upsilon_q \rho_q \vec{u}_q) + \nabla \cdot \left(\upsilon_q \rho_q \vec{u}_q \vec{u}_q\right) = -\upsilon_q \nabla \cdot P + \nabla \bar{\bar{\tau}}_q + F_{\text{int}erfacial} + F_{external} \tag{2}$$

This system of equations is constrained by the fractional sum of the hold up: $\sum_{i=1}^{n} \upsilon_q = 1$. Here, υ_q, ρ_q, $\bar{u}_q$, represent, respectively, density, volume fraction, time–averaged velocity, P is pressure, $F_{\text{int}erfacial}$ (e.g. drag force, lift force and added mass forces, i.e., virtual mass and close-to-wall lift and lubrication forces) is the averaged interfacial momentum transfer between the phases, $F_{external}$ is the gravitational acceleration, and $\nabla \bar{\bar{\tau}}_q$ the shear stress tensor.

$$\bar{\bar{\tau}}_q = \mu_{eff}\left(\nabla\vec{u}_q + \left(\nabla\vec{u}_q\right)^T - \frac{2}{3}I\nabla\cdot\vec{u}_q\right) \tag{3}$$

Where the liquid phase effective viscosity, μ_{eff} is composed of two contributions: the molecular viscosity $\mu_{L,L}$, and the shear induced turbulent viscosity $\mu_{L,Tur}$

$$\mu_{L,eff} = \mu_{L,L} + \mu_{L,Tur}, \tag{4}$$

The gas phase effective viscosity is calculated from the effective liquid viscosity

$$\mu_{G,eff} = \mu_{L,eff}\frac{\rho_G}{\rho_L}. \tag{5}$$

The shear-induced turbulent viscosity in the liquid phase is calculated using the k-ε [11]. In this two-equation model, the turbulence length and time scales are developed from the turbulent kinetic energy (k) and dissipation rate (ε) which are obtained from separate modeled transport equations. Reynolds stresses are related to the mean rate of strain through a turbulent viscosity, $\mu_{L,Tur}$

$$\mu_{L,Tur} = C_\mu\rho_L\frac{k_L^2}{\varepsilon_L} \tag{6}$$

The governing differential equations for the turbulent kinetic energy (k) and its energy dissipation rate (ε) are calculated from their conservation equations (7, 8).

$$\frac{\partial\left(\upsilon_L\rho_L k_L\right)}{\partial t} + \nabla\cdot\left(\upsilon_L\rho_L k_L\vec{u}_L - \upsilon_L\left(\mu_{L,L} + \frac{\mu_{L,L}}{\sigma_k}\right)\nabla k_L\right) = \varepsilon_L\left(G_L - \varepsilon\rho_L\right) \tag{7}$$

$$\frac{\partial(\upsilon_L \rho_L \varepsilon_L)}{\partial t} + \nabla \cdot \left(\upsilon_L \rho_L \varepsilon_L \vec{u}_L - \upsilon_L \left(\mu_{L,L} + \frac{\mu_{L,Turb}}{\sigma_\varepsilon} \right) \nabla \varepsilon_L \right) =$$
$$-\nabla \left(\upsilon_L \frac{\mu_{L,eff}}{\sigma_\varepsilon} \nabla \varepsilon_L \right) + \upsilon_L \frac{\varepsilon_L}{k} (C_{\varepsilon 1} G_L - C_{\varepsilon 2} \varepsilon_L \rho_L) \tag{8}$$

The production of turbulent kinetic energy G_L is expressed in terms of the velocity gradients and the turbulent viscosity.

$$G_L = \upsilon_L \left(\nabla \vec{u}_l + \left(\nabla \vec{u}_l \right)^T \right) : \nabla \vec{u}_l \tag{9}$$

The model has five empirical constants, which are assigned these following values

$C_\mu = 0.09;$ $C_1 = 1.44;$ $C_2 = 1.92$ $\sigma_k = 1.0$ $\sigma_\varepsilon = 1.217$

The constants σ_k and σ_ε are turbulent Prandtl numbers for the diffusive transport for (k) and (ε).

2.2 Interphase Momentum Transfer

At the interface, the existence of two velocity fields between the two phases, leads to interfacial momentum transfer that can be attributed to the sum of independent interfacial forces such as the Magnus effect, Basset effect, drag force, lift force, lubrication, virtual mass force, and turbulent dispersion forces among others.

$$F_{interfacial} = f_{drag} + f_{lift} + f_{lubrication} + f_{VM} + f_{TD} + \ldots \tag{10}$$

The interface separating the two phases, is the most significant parameter in two-phase flow modeling, it provides the phenomenological criteria to define the flow regime. The interfacial forces between two phases are equal and opposite, so the net interfacial forces sum to zero. The geometry of the interfaces between two-phases determines the transport mechanisms between the

flows regimens, where two or more flow regimes can exist simultaneously in a single system.

Grace and Weber [2] established a relationship between flow regime and bubble geometry by mapping particle Reynolds number against Eötvös number for different systems with fixed value of the Morton number. At sufficiently low particle Reynolds numbers, the flow regime is considered viscous and the bubbles take on a spherical geometry. For intermediate o Allen's regime, the flow is classified as the viscous regime where the drag is attributed to viscous and inertial forces, and the bubbles become ellipsoidal shape. In the Newton's Regime, drag is due almost entirely due to inertial forces, is considered to be independent of particle Reynolds number.

For the two-fluid model, the averaged macroscopic velocity fields of the two phases are not independent of each other; the interfacial momentum transfer interactions between the two phases should be specified in order to close the momentum conservation equation and, to determine with reasonable accuracy the overall flow characteristics and gas hold-up. The resulting interaction forces are approximated through semi- empirical correlations, that are functions of dimensionless numbers Grace [2], the bubble Reynolds (Re_b), number, Eötvös (E), Morton numbers (M) and Weber number (We) which are defined as follows:

$$\mathrm{Re}_b = \frac{\rho_l d_b |u_b - u_l|}{\mu_l} \qquad Eo = \frac{\rho_l d_b^2}{\sigma} \qquad M = \frac{g\mu_l^4}{\rho_l \sigma^3} \qquad We = \frac{\rho_l |u_b - u_l|^2}{\sigma} \tag{11}$$

($\rho_g \leq \rho_l$, therefore $\Delta\rho \approx \rho_l$), σ is the surface tension, these dimensionless number are used to characterize the shape of bubbles or drops moving in a surrounding fluid or continuous phase.

In this work only three contributions are taken into account, the drag force, lift and turbulence dispersion forces. The virtual mass force is caused by the relative acceleration between phases, and it is considered to be negligible if the density of the disperse phase is much larger than the density of the continuum phase. Previous works [5,6] report that in the case of bubble column this force has a very small effect on the interphase momentum transfer.

2.2.1 Drag Force

The drag force is a measure of the equilibrium relative velocity between phases, a moving bubble in a liquid is slowed down by the surrounding liquid and simultaneously part of the surrounding liquid is accelerated. The drag force is the most predominant interfacial closures in the momentum transfer. The liquid drag force and, f_D, acting on the bubble under steady-state conditions is given in terms of the dimensionless drag coefficient C_d based on the relative velocity o slip velocity:

$$f_D = -\frac{3}{4}\upsilon_g \rho_L \frac{C_D}{d_P}\left|\bar{u}_g - \bar{u}_L\right|\left(\bar{u}_g - \bar{u}_L\right) \tag{12}$$

ρ_l is the density of the continuous phase, d_b , the effective bubble diameter, i.e. diameter of a sphere having the same volume as the dispersed element without deformation on the projected area in the flow direction, $\left(\bar{u}_g - \bar{u}_L\right)$ the relative velocity also known as the slip velocity.

In the literature there are many developed empirical and semispherical correlation that

describe the drag forces acting on a single bubbles. The values of the drag coefficient are generally obtained from single bubble terminal velocities measurements, as a function of operating conditions. It is important, to knows the limitations of a given model and its range of validity prior to using it. For air-water system, the Ishii and Zuber and Grace models [1,2] are extensively used and are implemented in this study to establish their capability in determining experimental air hold-up.

Ishii-Zuber model

The Ishii-Zuber local drag correlations [1] for dispersed two-phase flows were developed from mixture viscosity model and simple similarity criteria. For a dense system, increased effective mixture viscosity is attributed to increased bubble concentrations and is reflected with an increased drag. Supposing maximum packing, a power law correlation for effective mixture viscosity is obtained by the following equation:

$$\mu_m = \mu_c \left(1 - \frac{\upsilon}{\upsilon_{\max}}\right)^A \tag{13}$$

where $\upsilon_{\max}$ take on the value of 0.62 for solid and ranges between 0.95 and 1 for fluid, and the exponent A is related to the mixture viscosity as follow:

$$A = -2.5\upsilon_{\max}\left(\frac{0.4\mu_c + \mu_d}{\mu_c + \mu_d}\right) \tag{14}$$

This mixture viscosity is then used to define mixture Reynolds number.

$$\mathrm{Re}_m = \frac{\rho_l d_b \left|u_b - u_l\right|}{\mu_m} \tag{15}$$

At sufficiently low Reynolds numbers, the flow regime is viscous and bubbles are spherical, the drag coefficient is approximated by the Schiller-Naumann type correlation.

$$C_{D,Sphere} = \frac{24}{\mathrm{Re}_m}\left(1 + 0.1\mathrm{Re}_m^{\,0.75}\right) \qquad 0 \le \mathrm{Re}_m \le O(1000) \tag{16}$$

For a dilute spherical regime, the Re_m is replaced by particle Reynolds number, Re_p, and the same correlation is used. For intermediate o Allen's regime, the flow is classified as the viscous Newton's regime, the surface tension effects become significant and the bubbles develop ellipsoidal shape.

$$C_{D,Ellips} = C_{D\infty} = \frac{2}{3}Eo^{1/2} \qquad O(10^3) \le \mathrm{Re}_m \le O(10^5) \tag{17}$$

For a dense system,

$$C_D^{Dense} = C_{D\infty}\left[\frac{1 + 17.67\, f(\upsilon_g)^{6/7}}{18.67\, f(\upsilon_g)}\right] \tag{18}$$

$$f(\upsilon_g) = \frac{\mu_l}{\mu_m}(1 - \upsilon_g)^{\frac{1}{2}} \tag{19}$$

An additional increase in the bubble diameter, the drag coefficient fall into spherical cap or Churn turbulent regime:

$$C_{D,cap} = C_{D\infty} = \frac{3}{8} \qquad O(10^3) \le \mathrm{Re}_m \le O(10^5) \tag{20}$$

While for the dense spherical cap regime, the drag coefficient becomes

$$C_{D,Ellips} = C_{D\infty}(1 - \upsilon_g)^2 \tag{21}$$

This drag law characterizing the motion of bubbles, drops, and particles in various dispersed

two-phase flows under steady state and adiabatic conditions previously indicated satisfactory agreements at wide ranges of the concentration and Reynolds number.

Grace model

Grace drag correlation [2] is developed for air-water bubbly flows, and yield good results for air-water systems, is valid for wide range of *Re*, has been considered to provide good approximations for drag coefficient it consists of piecewise functions valid for different *Re*. The equivalent to Ishii Zuber for ellipsoidal particle regime

$$C_D^{Ellipse} = \frac{4}{3}\frac{g \cdot d_p \cdot \Delta\rho}{U_T^2 \cdot \rho_L} \tag{22}$$

Terminal velocity UT is given by:

$$U_T = \frac{\mu_L}{\rho_L \cdot d_p} \cdot M^{-0.149} \cdot (J - 0.857) \tag{23}$$

Where M is Morton Number is expressed as:

$$M = \frac{g\mu_l^4}{\rho_l \sigma^3} \tag{24}$$

$$\begin{cases} J = 94 \cdot H^{0.751} & 2 < \mathrm{H} < 59.3 \\ J = 3.42 \cdot H^{0.441} & \mathrm{H} > 59.3 \end{cases} \tag{25}$$

$$H = \frac{4}{3} \cdot E_0 \cdot M^{-0.149} \cdot \left(\frac{\mu_L}{\mu_{ref}}\right) \qquad \mu_{ref} = 0.0009 \frac{kg}{m \cdot s} \tag{26}$$

where μ_{ref} is the molecular viscosity of water at reference temperature and pressure (25 ºC and 101.325 kPa).

This drag correlation described so far is valid for a single dispersed bubble in an infinite medium. To account for high particle concentrations, the single bubble Grace drag coefficient in dilute disperse phase regime, $C_{D\infty}$, is extended to describe the effect of neighboring bubbles by using power-law approximation:

$$C_D^{Dense} = \upsilon_l^p C_{D\infty} \tag{27}$$

For dense flows, the exponent is a tuning parameter and, its value is bubble size dependent

2.2.2 The lift force (f_L)

These lift force (f_L) is caused by the effect of the pressure and stress over the bubble surface and is the principal mechanism that determines the phase distribution in bubble flow. The transversal lift force acting on a spherical particle due to fluid velocity shear can be expressed as:

$$f_L = C_L \upsilon_g \rho_L \left(\vec{u}_g - \vec{u}_L\right) \times \nabla \times u_L \tag{28}$$

where C_L is the lift coefficient, is in the range 0.1 and 0.5 for viscous liquid. The sign of this force depends on the orientation of slip velocity with respect to the gravity vector, $\left(\vec{u}_g - \vec{u}_L\right)$ is the slip velocity.

2.2.3 The turbulent dispersion force

The effect of disperse phases eddies in the continuum phase are represented in the turbulent dispersion force. There exist many ways in modeling the turbulent dispersion force, but one of the most often used in these bubble column systems is Lopes de Bertodano´s model [12].

$$f_{TD} = -C_{TD}\rho_L k_{TD}\nabla \upsilon_L \tag{29}$$

where C_{TD} , is the turbulent dispersion coefficient and its recommended range is between 0.1 and 0.5, is not universal, a required value of 500 for small bubbles, where k_{TD} is the liquid turbulent kinetic energy per unit of mass.

2.3 Physical Problem

In the current work the hydrodynamics of Pironti experimental set-up [3] is used, it converts pressure drop into air holdup. Figure 1 is a schematic overview of the investigated column. The column has a draft tube. The bubble column was employed in semi-batch mode, and was filled with tap water. And, then air was introduced in the column at the bottom of the conical section through a nozzle with internal diameter of 0.0063 m. All the measures were taken a 25° Celsius and atmospheric pressure. The bubble column has two regions: (a) a conical base; and (b) a cylindrical region. The height of the cylindrical region is 3 m long, with an internal diameter of 0.15 m. The draft tube is 2 m long, with a diameter of 0.07 m and 0.005 m of thickness. The conic section has a height of 0.43 m and an angle of 34°. The draft tube was located 0.2 m above the column entry. The superficial gas velocity is 0.05 m/s.

Mesh Sensitivity Analysis

For the numerical analysis, the domain was discretized with a mesh chosen to guarantee a difference in pressure drop of less than 5 % for a sequential 50% of refinement. The physical properties can be found in table 1. Simulation is carried out by using a finite element-based finite volume numerical scheme together with a coupled solution algorithm (ANSYS-CFX). A typical run simulation took about 2 hours in a 1.6 GHz Intel core 2 duo processor and 1 GB RAM PC. As can be seen from the Fig 2, to determine the hold-up, finer mesh was not needed.

3. Results

Numerical results from Reynolds-averaged Navier-Stokes (RANS) and k-ε models are used to compare with Pironti experimental data [3]. The spouted column simulation provides a qualitative agreement with the observed experimental behavior and the expected hydrodynamic flow characteristics in the conical and exit sections of the draft tube. Based on results with k-ε, the flow reflects the high mixing and turbulence in the entry of the cone Fig 3(a-d).

The spouted flow or fountain region in the exit section of the draft tube is also well represented Fig. 3 (a-d). In the internal loop, the expected jet is formed, and this effect produces a global recirculation motion, in which the phases rise in the draft tube and descend through the annular region. Also, the momentum exchange is qualitatively characterized by equally balanced free-wall turbulence as the k-ε turbulence model captured well the main features of the mixing

region. The simulation that qualitatively best depicts these phenomena is the k-ε turbulence model with Ishii-Zuber drag force, case (d) Fig. 3 and Fig. 4.

The experimental air hold-up of 14.70 characterizes a broad range of flow parameters by a characteristic uniform equivalent bubble diameter of 6mm (monodispersed bubbly flow), under this conditions the phenomena of coalescence and break–up is less probable. The physical properties of the system, turns the interfacial force closures into a function of the bubble Reynolds number (Re), the Eötvös number (Eo). For the studied cases, the operating Eötvös and Morton numbers are 4.82 and 1.58e-11, respectively are defined a priori supposing constant transport properties for the uniform equivalent bubble diameter of 6mm, and the determined Reynolds number, $1140 \leq \mathrm{Re}_m \leq 1395$, is indicative of ellipsoidal flow regime. In this distorted bubble regime, the drag coefficient is approximately constant, $1.04 \leq C_D \leq 1.47$, is independent of Reynolds number, but dependent on particle shape through the dimensionless group known as the Eötvös number. The almost uniform Re, of equal–sized bubbles is characteristic of decreasing rise velocity.

Table 2, shows the results for k-ε two-equation turbulence closure used with: (A)-(D) only the Grace correlation with varying exponent p; (E)-(H) adding the lift force; and (I)-(N) adding simultaneously the lift and Lopes de Bertodano´s turbulent dispersion force. These results indicated that, for air-water system within a spouted column, a small positive exponent value (p= 0.5) should be used in order to predict a better drag coefficient and to capture experimental air

hold-up and flow behavior with Grace drag model. Furthermore, the exponent (p) of Grace drag correlation, could be as significant as the well established added effect of interfacial force closures (lift forces and turbulent dispersion force). This can shown when comparing, cases (A to D), Grace drag model alone, and decreasing p from 4 (C_{drag} =1.11) to p=0.5 (C_{drag} =1.04), the absolute error decreased from 36.75 to 15.20% for the determined air hold up. While, comparing cases (D), only Grace drag model with p= 0,5 (C_{drag} =1.04) with case (I) all interfacial closures included (p= 4, C_{drag} =1.32), C_{lift}=0.2, C_{TD}=0.1), the absolute error also decreased from 36.75 to 15.04% for the determined air hold up, this is indicative of the importance of tuning the p parameter in the drag force for the Grace correlation.

In table 3, the Ishii-Zuber drag model and Grace adjusted drag model, are compared for their capability to match experimental gas hold- up using k-ε two-equation turbulence closure: (O)-(P) Grace with the best exponent (p=0.5) against the Ishii-Zuber; (Q)-(R) adding the lift force; and (S)-(T) adding simultaneously the lift and Lopes de Bertodano´s turbulent dispersion force Numerical results of Reynolds-averaged Navier-Stokes equations when compared with Pironti at al. experimental data indicated that both drag models, predicted the air hold-up within experimental error. Ishii-Zuber liquid-gas drag model consistently provided better agreement of experimental results; it correctly determines the hold up within 0.1%. Numerical agreement with adjusted Grace liquid-gas drag model, is exponent dependent $(4 \le p \le -1)$, $p = 0.5$ determined the best hold up within 0.4% under the following interphase momentum closure (C_{drag} =1.30, C_{lift}=0.2, C_{TD}=0.2). The added effect of the interphase forces (e.g. drag force, lift force and

turbulent dispersion forces), and the k-ε turbulence model, in the CFD modeling of the air-water system in the spouted bed effectively improved the prediction of the air hold up. The absolute error decreased from 18.69 to 0.14% under the following interphase momentum closure (C_{drag} =1.32, C_{lift}=0.2, C_{TD}=0.2) when Ishii-Zuber drag closure is used, while a decrease from 15.20 to 0.44% is attained with the Grace Drag closure.

4. Concluding Remarks

Two fluid CFD simulation with k-ε turbulence closure explored the capabilities of Ishii-Zuber and Grace drag closures [1,2], in the correct determination of the air hold-up. The momentum exchange is quantitatively described by equally balanced free-wall turbulence as the k-ε turbulence models portray well the main aspect of the mixing region. Numerical results of Reynolds-averaged Navier-Stokes equations with k-ε two-equation turbulence closures models when compared with Pironti experimental data [3] indicated that both drag models, predicted the air hold up within experimental error. Furthermore, Ishii-Zuber liquid-gas drag model consistently provided better agreement of experimental results; it correctly determines the hold up within 0.14% under the following interphase momentum closure (C_{drag} =1.32, C_{lift}=0.2, C_{TD}=0.2) Numerical agreement with adjusted Grace liquid-gas drag model is exponent dependent $(4 \le p \le -1)$, it improved as the exponent decreased, for $p = 4$ the determined hold up is within 14% while for $p = 0.5$ determined hold up is within 0.44%, under the following interphase momentum closure (C_{drag} =1.30, C_{lift}=0.2, C_{TD}=0.2) . The results confirmed that, the drag

models are very important however by themselves do not suffice in the modeling of the quantitative features of the mixing flow. In fact, when lift and turbulence dispersion forces were included, errors decreased in the quantitative prediction, from 18% to 0.14% for Ishii-Zuber and 15% to 4% for Grace.

Acknowledgments

The authors wish to thank the DID of Simón Bolívar University, and the FONACIT of Venezuela, for their continuing support of the three participating Research Groups.

References

[1] Ishii M., Zuber N., Drag coefficient and relative velocity in bubbly, droplet or particulate flows, AIChE Journal, **25** (1979), 843-855.

[2] Clift, R., J. R. Grace, and M. E. Weber, Bubbles, Drops and Particles, Academic Press, New York (1978).

[3] Pironti F.F., Medina V.R., Calvo R. and Sáez A.E., Effect of draft tube position on the hydrodynamics of a draft tube slurry bubble column, Chemical Engineering Journal, **60** (1995), 155-160.

[4] Joshi, J. B., "Computational Flow Modelling and Design of Bubble Column Reactors," Chem. Eng. Sci., **56** (2001), 5893.

[5] Zhang, D., Deen, N.G and Kuipers, J.A.M, Numerical simulation of the dynamic flow

behavior in a bubble column: A study of closure for turbulence and interface forces, Chemical Engineering Science, **61** (2006), 7593-7608.

[6] Tabid, M., Roy, S. and Joshi, J., CFD simulation of bubble column- An analysis of interphase forces and turbulence models, Chemical Engineering Science, **139** (2008), 589-614.

[7] Riera, J., Zeppieri, S., Rojas-Solorzano, L. and Derjani-Bayeh, S., CFD Simulation of Air Water in a spouted bed, Chemical Engineering Transations, accepted for publication, february 2011.

[8] Ekambara, K., Dhotre, M. and Joshi, J., CFD simulations of bubble column reactors: 1D, 2D and 3D approach, Chemical Engineering Science, **6** (2005), 6733-6746.

[9] Jakobsen, H., Lindborg, H. and Dorao, C., Modeling of Bubble Column Reactor: Progress and Limitations, Industrial and Engineering Chemistry Research, **44** (2005), 5107-5151.

[10] A. Sokolichin, G. Eigenberger, Simulation of buoyancy driven bubbly flow: established simplifications and open questions, AIChE J. **50** (2004), 24–45.

[11] Launder, B.F. and Spalding, D.B, The numerical computation of turbulence, Academic, New York, 1974.

[12] Lopes de Bertodano M., Turbulent bubble flow in a triangular duct. Ph.D. Thesis Rensselaer Polytechnic Institute. Troy New York, 1991.

Table 1: Physical properties used for the numerical simulations

Bubble Phase (Air)	Viscosity	$1.831 \times 10^{-5}\ kg/m.s$
	Density	$1.865\ kg/m^3$
	Bubble Diameter	$6 \times 10^{-6}\ m$
Continuous Phase (Water)	Viscosity	$9 \times 10^{-4}\ kg/m.s$
	Density	$997\ kg/m^3$
	Surface Tension	$7.3 \times 10^{-3}\ N/m$
	$E = g\Delta\rho d^2{}_e/\sigma$	4.82 Dimensionless
	$M = g\mu^4\Delta\rho/\rho^2\sigma^2$	1.58×10^{-11} Dimensionless

Table 2: Error (%) in air hold up Momentum transfer modeling with grace drag force, k-ε model Turbulence Closure

Case	Exponent , p Drag model	$C_{Ave,Drag}$	C_{lift}	C_{TD}	Re_p	Error (%)
A	4.0	1.11	0	0	2079	36.75
B	2.0	1.20	0	0	1687	36.75
C	1.0	1.29	0	0	1273	34.15
D	0.5	1.04	0	0	1275	15.20
E	4.0	1.08	0.2	0	1914	32.48
F	2.0	1.25	0.2	0	1785	32.48
G	1.0	1.35	0.2	0	1692	10.31
H	0.5	1.31	0.2	0	1440	1.92
I	4.0	1.32	0.2	0.1	1598	15.04
J	2.0	1.29	0.2	0.1	1718	27.89
K	1.0	1.22	0.2	0.1	1456	1.39
L	0.5	1.30	0.2	0.1	1395	0.44
M	0.1	1.32	0.2	0.1	1357	3.92
N	-0.5	1.53	0.2	0.1	1350	3.97

Table 3: Effect of Interface drag forces on air hold up with k-ε Turbulence closure

Case	Drag model	$C_{Ave,Drag}$	C_{lift}	C_{TD}	Re_p	Error (%)
O	Ishii-Zuber	1.47	0	0	1159	18.69
P	Grace p=0.5	1.04	0	0	1275	15.20
Q	Ishii-Zuber	1.47	0.2	0	1114	0.18
R	Grace p=0.5	1.31	0.2	0	1440	1.92
S	Ishii-Zuber	1.32	0.2	0.1	1086	0.14
T	Grace p=0.5	1.30	0.2	0.1	1395	0.44

Fig. 1: Pironti et al (1995) experimental set up [3].

Fig. 2: Conical section meshing.

Fig. 3: Conical section mixing: For all cases, the closures are: C_{lift}=0.2, C_{TD}=0.2, a) Grace: p=4, C_{drag} =1.04 b) Grace: p=0.5 , C_{drag} =1.30 c) Grace: p=0.1, C_{drag} =1.31 d) Ishii-Zuber, C_{drag} =1.32.

Fig. 4: Spout bed exit section mixing: For all cases, the closures are: C_{lift}=0.2, C_{TD}=0.2, a) Grace: p=4, C_{drag} =1.04 b) Grace: p=0.5 , C_{drag} =1.30 c) Grace: p=0.1, C_{drag} =1.31 d) Ishii-Zuber, C_{drag} =1.32.

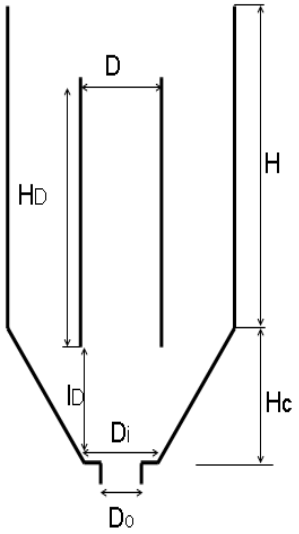

Figure 1

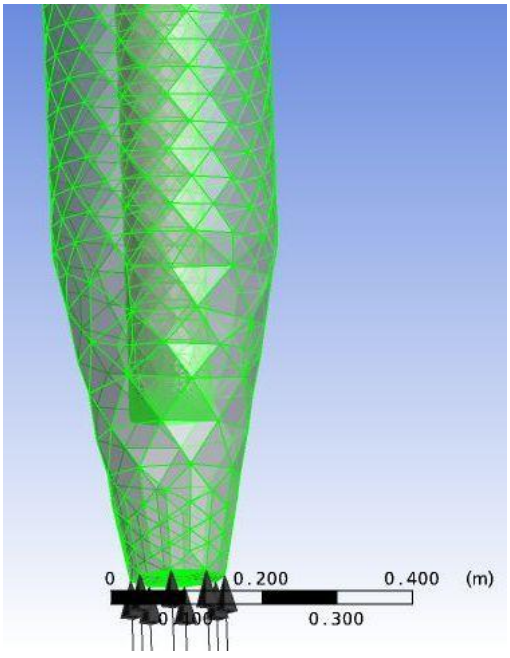

Figure 2

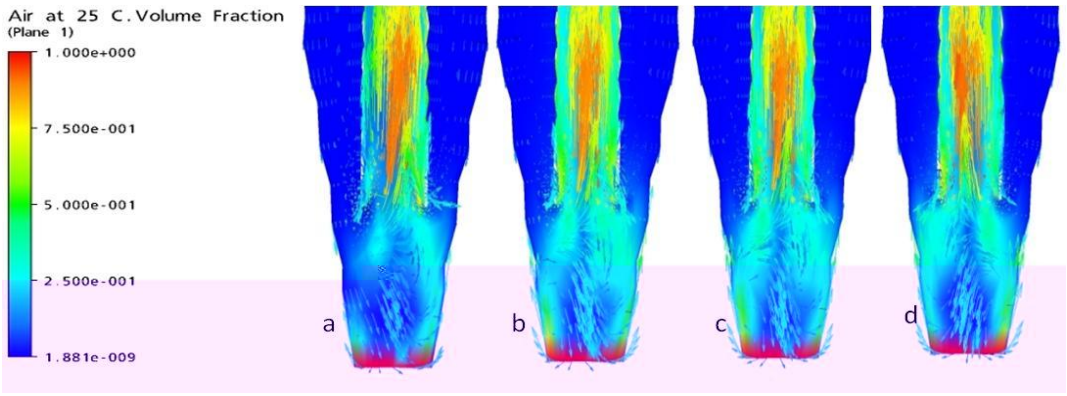

Figure 3

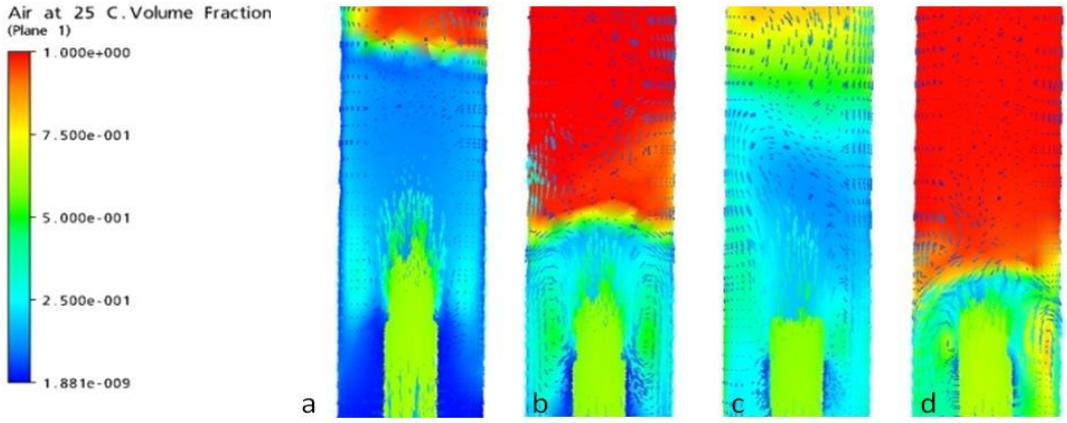

Figure 4